CRB1-Associated retinal dystrophies: a anticipation of future clinical trials

Nguyen, X.T.A.; Talib, M.; Schooneveld, M.J. van; Wijnholds, J.; Genderen, M.M. van; Schalij-delfos, N.I.E.; ... ; Boon, C.J.F.

CRB1-Associated Retinal Dystrophies: A Prospective Natural History Study in Anticipation of Future Clinical Trials

XUAN-THANH-AN NGUYEN, MAYS TALIB, MARY J. VAN SCHOONEVELD, JAN WIJNHOLDS, MARIA M. VAN GENDEREN, NICOLINE E. SCHALIJ-DELFOS, CAROLINE C.W. KLAVER, HERMAN E. TALSMA, MARTA FIOCCO, RALPH J. FLORIJN, JACOLINE B. TEN BRINK, FRANS P.M. CREMERS, MAGDA A. MEESTER-SMOOR, L. INGEBORGH VAN DEN BORN, CAREL B. HOYNG, ALBERTA A.H.J. THIADENS, ARTHUR A. BERGEN, AND CAMIEL J.F. BOON

• PURPOSE: To investigate the natural disease course of retinal dystrophies associated with crumbs cell polarity complex component 1 (*CRB1*) and identify clinical end points for future clinical trials.

• DESIGN: Single-center, prospective case series.

• METHODS: An investigator-initiated nationwide collaborative study that included 22 patients with *CRB1*-associated retinal dystrophies. Patients underwent ophthalmic assessment at baseline and 2 years after baseline. Clinical examination included best-corrected visual acuity (BCVA) using Early Treatment Diabetic Retinopathy Study charts, Goldmann kinetic perimetry (V4e isopter seeing retinal areas), microperimetry, full-field electroretinography, full-field stimulus threshold (FST), fundus photography, spectral-domain optical coherence tomography, and fundus autofluorescence imaging.

• RESULTS: Based on genetic, clinical, and electrophysiological data, patients were diagnosed with retinitis pigmentosa (19 [86%]), cone-rod dystrophy (2 [9%]), or isolated macular dystrophy (1 [5%]). Analysis of the entire cohort at 2 years showed no significant changes in BCVA ($P = .069$) or V4e isopter seeing retinal areas ($P = .616$), although signs of clinical progression were present in individual patients. Macular sensitivity measured on microperimetry revealed a significant reduction at the 2-year follow-up ($P < .001$). FST responses were measurable in patients with nonrecordable electroretinograms. On average, FST responses remained stable during follow-up.

• CONCLUSION: In *CRB1*-associated retinal dystrophies, visual acuity and visual field measures remain relatively stable over the course of 2 years. Microperimetry showed a significant decrease in retinal sensitivity during follow-up and may be a more sensitive progression marker. Retinal sensitivity on microperimetry may serve as a functional clinical end point in future human treatment trials for *CRB1*-associated retinal dystrophies. (Am J Ophthalmol 2022;234: 37–48. © 2021 The Authors. Published by Elsevier Inc. This is an open access article under the CC BY license (http://creativecommons.org/licenses/by/4.0/))

AJO.com Supplemental Material available at AJO.com.

Accepted for publication July 15, 2021.

From the Department of Ophthalmology (X.-T.-A.N., M.T., J.W., N.E.S.-D., H.E.T., C.J.F.B.), Leiden University Medical Center, Leiden, the Netherlands; Department of Ophthalmology (M.J.v.S., C.J.F.B.), Amsterdam University Medical Center (UMC), Academic Medical Center, Amsterdam, the Netherlands; The Netherlands Institute for Neuroscience (NIN-KNAW) (J.W., A.A.B.), Amsterdam, the Netherlands; Bartiméus Diagnostic Centre for Complex Visual Disorders (M.M.v.G., H.E.T.), Zeist, the Netherlands; Department of Ophthalmology (M.M.v.G.), University Medical Centre Utrecht, Utrecht, the Netherlands; Department of Ophthalmology (C.C.W.K., M.A.M.-S., A.A.H.J.T.); Department of Epidemiology (C.C.W.K.), Erasmus University Medical Center, Rotterdam, the Netherlands; Department of Ophthalmology (C.C.W.K., C.B.H.), Radboud University Medical Center, Nijmegen, the Netherlands; Institute for Molecular and Clinical Ophthalmology (C.C.W.K.), Basel, Switzerland; Mathematical Institute (M.F.), and Department of Biomedical Data Sciences (M.F.), Leiden University Medical Center, Leiden, the Netherlands; Department of Clinical Genetics (R.J.F., J.B.t.B., A.A.B.), Amsterdam University Medical Center (UMC), Academic Medical Center, Amsterdam, the Netherlands; Department of Human Genetics and Donders Institute for Brain, Cognition and Behaviour (F.P.M.C.), Radboud University Medical Center, Nijmegen, the Netherlands; Rotterdam Eye Hospital (L.I.v.d.B.), Rotterdam, the Netherlands

Inquiries to Camiel J.F. Boon, Department of Ophthalmology, Leiden University Medical Center, Postal Zone J3-S, Albinusdreef 2, 2333 ZA Leiden, Netherlands; e-mail: c.j.f.boon@lumc.nl

A WIDE RANGE OF RELATED RETINAL DYSTROPHIES (RDs), including Leber congenital amaurosis (LCA), retinitis pigmentosa (RP), and cone(-rod) dystrophies (CRDs), can be caused by variants in the crumbs cell polarity complex component 1 (*CRB1*) gene.[1-4] LCA is considered the most severe RD, presenting at birth or early infancy, and is characterized by severe visual impairment, nystagmus, poor pupillary responses, and absent responses on electroretinography.[4] RP is characterized by primary degeneration of rod photoreceptors with secondary cone degeneration. Initial symptoms in RP typically include night blindness due to degeneration of the rods, followed by concentric visual field loss and, eventually, central vision loss later in life due to cone dysfunction.[5] RP comprises a broad spectrum of phenotypic presentations and can become symptomatic at different

0002-9394/$36.00
https://doi.org/10.1016/j.ajo.2021.07.021

ages, ranging from early childhood (ie, juvenile RP) to middle age, caused by a broad spectrum of genes.[6]

The *CRB1* gene encodes the transmembrane protein crumbs homologue 1 (CRB1), which, in mammals, localizes to the subapical region of Müller and photoreceptor cells.[7-10] The canonical isoform of CRB1 consists of 19 epidermal growth factor domains, 3 laminin A globular-like domains, and a short cytoplasmic tail that contains FERM/PDZ binding motifs.[11] Recently, a novel isoform of CRB1, CRB1-B, was also discovered, which is presumed to be more abundant in the human retina than its canonical form.[12]

While the function of CRB1 in the human retina has not been fully elucidated, it has been suggested to play a key role in cell polarity, cell-to-cell adhesion, photoreceptor morphogenesis, and retinal maturation.[8,13-16] The role of CRB1 in retinal development is supported by the abnormal thickening and coarse lamination of the inner retinal layers that has been described in most cases of *CRB1*-associated RDs, which strikes a resemblance to an immature retina.[17] Other clinical features described in *CRB1*-associated RDs include hyperopia, optic nerve drusen, preservation of para-arteriolar retinal pigment epithelium, cystoid macular edema, nummular pigmentation, and Coats-like exudates.[18]

Currently, no treatment exists for patients with *CRB1*-associated RDs, but proof-of-concept of adeno-associated virus-mediated gene transfer was achieved using murine models.[15,19] As *CRB1* gene therapy is being developed, it is crucial to determine adequate clinical end points ahead of these upcoming trials.[10] This requires an optimal understanding of the disease, its variability, and its progression, based on retrospective and prospective natural history studies.[20] A retrospective study previously performed by our study group provided insights into the progressive decline in visual acuity and visual fields in patients with *CRB1* variants, showing that the optimal window for treatment is likely within the first 2 to 3 decades of life based on these outcome measures.[18] However, our knowledge about the feasibility of other psychophysical outcome measures, such as microperimetry and full-field-stimulus thresholds, remains limited.[18,21]

Here we report the first prospective natural history study performed in patients with biallelic *CRB1* variants. The objective of this study was to describe the disease progression in *CRB1*-associated retinal dystrophies and to determine potential clinical end points in anticipation of future therapeutic trials. Based on these findings, we provide the first recommendations and considerations for the study design of upcoming *CRB1* clinical trials.

METHODS

• **PATIENT RECRUITMENT:** This nationwide collaborative study recruited patients from 2 different registries: the RD5000 database, a national registry for inherited retinal diseases, and the Delleman archive for genetic eye diseases at Amsterdam University Medical Center.[22] Inclusion criteria for this study were the presence of biallelic *CRB1* variants with a RD phenotype, and a best-corrected visual acuity (BCVA) of ≥20/400 Snellen acuity. The study included 22 patients with biallelic *CRB1* variants, of which 10 patients (45%) originated from a previously described genetically isolated population.[21,23] Patients were examined at baseline and 2 years after baseline at Leiden University Medical Center.

The study protocol, genetic findings, and baseline characteristics of the included patients have been described in detail elsewhere and are briefly described here.[24] The current study presents the 2-year follow-up data and describes the longitudinal findings in this cohort.

The study protocol was approved by the Erasmus Medical Center Medical Ethics Committee, as it was performed within the framework of the RD5000, and from the Leiden University Medical Center Review Board. Informed consent was obtained from individuals and/or legal guardians, and the study adhered to the tenets of the Declaration of Helsinki.

• **CLINICAL EXAMINATION:** Refraction and BCVA were measured monocularly, using the Early Treatment Diabetic Retinopathy Study (ETDRS) letter chart. ETDRS letters were converted to logMAR values for statistical analysis. Visual fields (V4e isopter) were obtained using Goldmann perimetry, which were subsequently converted to digital seeing retinal areas (in mm^2) using a method described by Dagnelie.[25] A change ≥20% in retinal seeing area was considered clinically significant based on previous test-retest reliability studies in patients with RP.[26] Macular sensitivity was assessed by macular integrity assessment (MAIA) microperimetry (CenterVue) using the standard 37-stimuli grid pattern under mesopic conditions. Fixation stability was quantified using the 95% bivariate contour ellipsoid areas (BCEA), which encompasses 95% of all the fixation points during examination. To minimize a learning effect, patients first underwent a practice session (fixed strategy) before formal testing using the 4-2 threshold strategy.[27,28] For follow-up measurements, the inbuilt follow-up software of the MAIA microperimetry was used, enabling accurate reassessment of the same test loci evaluated at baseline. If automatic alignment failed, manual alignment was performed using characteristic retinal landmarks.

After 30 minutes of dark-adaption, full-field electroretinography (ERG) responses were recorded on the Diagnosys using Dawson Trick Litzkow electrodes, which incorporated the International Society for Clinical Electrophysiology Standards (ISCEV). ERGs were only repeated at follow-up in patients with residual ERG function. A subset of patients underwent full-field stimulus threshold (FST; Diagnosys LLC) testing using white and chromatic stimuli with the reference luminance (0 dB) set to 0.01 candela

(cd)/m^2 (25 cd/m^2 presented for 4 milliseconds). Based on FST data from previous studies, the normal threshold for white stimuli, while accounting for differences in reference luminance, should be set at −53 dB.[29-31] Thresholds were measured in triplicate for each stimulus and were averaged per eye. Differences between averaged chromatic sensitivities were used to determine whether responses were rod-mediated (blue-red difference of >22 dB), cone-mediated (blue-red difference of <3 dB), or mixed rod- and cone-mediated (blue-red difference between 3 and 22 dB).[29,32]

Retinal imaging included fundus photography (Topcon TRC-50DX, Topcon Medical Systems, Inc), spectral-domain coherence tomography (SD-OCT; Spectralis), and 488-nm wavelength fundus autofluorescence (FAF; Heidelberg Engineering). On SD-OCT, the laminar organization of the inner retinal layers (inner limiting membrane through external limiting membrane) was categorized into 3 different grades: (1) normal organization without coarse lamination, (2) normal organization with coarse lamination, and (3) relative disorganization with coarse lamination.

In addition, the integrity of the external limiting membrane (ELM) and the ellipsoid zone (EZ) hyperreflective bands of the outer retina were evaluated at the parafovea (within 2.5 mm of the foveal center) and perifovea (outside 2.5 mm of the foveal center). The retinal bands were defined as continuous, discontinuous, or indiscernible. Overall definitions and examples of gradings of the inner and outer retina are provided in the Supplemental Figure. SD-OCT images were assessed by 2 authors (X.N. and M.T.) and reviewed by a third author (C.J.F.B.) in case of discrepancy between the 2 authors.

• **STATISTICAL ANALYSIS:** Data analysis was performed using R 3.6.2 software (R Foundation for Statistical Computing). The normality of data was analyzed using the Shapiro-Wilk test and was also visually plotted. Continuous data are presented as mean ± SD or range, in the case of normal distribution, and as median, interquartile range (IQR), and range, in the case of nonnormal distribution. Categorical data are presented as frequencies and percentages. Changes in parameters between baseline and follow-up were assessed using a linear mixed-effect model while accounting for paired eye data within patients. Correlation testing was performed with the Spearman correlation test, using data of the right eye only. The level of significance was set at 0.05. Bonferroni adjustments were applied for multiple testing where appropriate.

RESULTS

• **CLINICAL AND GENETIC CHARACTERISTICS:** The study assessed 22 patients, of which 10 (45%) originated from a previously described genetically isolated population, at baseline and at the 2-year follow-up.[24] A summary of the clinical findings in this cohort is provided in the Table and is also described for each patient individually in Supplemental Table 1. Patients were a median age of 25.7 years (IQR, 19.4; range, 6.2-74.8 years) at baseline, and the mean follow-up time was 2.04 ± 0.05 years (range, 1.97-2.19 years). Based on ERG patterns and clinical examination, a clinical diagnosis of RP (19 [86%]), CRD (2 [9%]), or macular dystrophy (1 [5%]) was made. The median self-reported age at onset was 3.0 years (IQR, 7.8; range, 0.8-49.0 years), and the median disease duration (age at onset subtracted from current age) was 18.7 years (IQR, 16.7; range, 4.7-39.3 years). An adult onset of symptoms was reported by 2 patients.

The cohort presented with 15 different *CRB1* variants, of which 12 were missense variants, 1 splice-site variant, 1 in-frame deletion, and 1 nonsense variant (Figure 1[24] and Supplemental Table 1). The most common variant found in this cohort was the founder variant c.3122T>C (p.Met1041Thr), which was present in a homozygous manner in all 10 patients from the genetic isolate and in a compound heterozygous manner in 1 patient from outside the isolate. In 10 of 11 patients (91%), including the patient from outside the isolate, this variant caused an early-onset RP phenotype. Patient P10 exhibited a late-onset CRD phenotype, despite originating from the genetic isolate. Targeted next-generation sequencing found no other variants in patient P10. Additionally, 2 patients with the variant p.(Thr631Cys) in a compound heterozygous manner showed relative preservation of visual function and retinal structure at later ages compared with other patients with RP in this cohort, which was suggestive for a milder form of RP.

• **VISUAL ACUITY AND REFRACTION:** The mean BCVA of the study eyes was 41.1 ± 18.3 ETDRS letters (range, 18.0-78.0 letters; equivalent to 0.88 logMAR or 20/150 Snellen) at baseline and 38.6 ± 19.7 ETDRS letters (range, 8.5-76.5 letters; equivalent to 0.93 logMAR or 20/170 Snellen) at the 2-year follow-up. A trend for a lower ETDRS score at follow-up was observed, but this finding was not statistically significant (−2.5 ETDRS letters, 95% CI, −5.2 to 0.2; $P = .069$). A loss of ≥15 ETDRS letters (ie, a loss of 3 ETDRS lines) was measured in 5 eyes of 5 patients (11%) at the 2-year follow-up, whose initial ages ranged from 22 to 31 years (Figure 2, A). In 2 of 5 eyes (40%) with a BCVA loss of ≥15 ETDRS letters, clinical examination showed significant posterior subcapsular cataract at both visits. Patient P1 underwent cataract surgery in both eyes between visits, with no improvement in BCVA. No new cases of cataract were seen at follow-up. Spherical equivalent of the refractive error, excluding pseudophakic patients, did not significantly change between visits (−0.09 diopter [D]; 95% CI, −0.34 to 0.15 D; $P = .455$).

• **KINETIC PERIMETRY AND MICROPERIMETRY:** The median size of V4e isopter seeing retinal areas, averaged between both eyes of each individual patient, was 176.0 mm^2

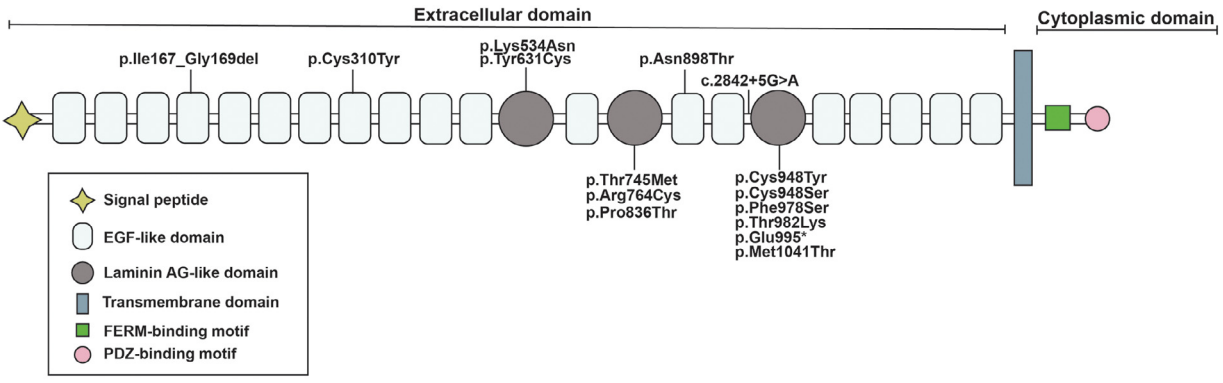

FIGURE 1. A schematic drawing of the crumbs homologue 1 (CRB1) protein structure and the variants found in our cohort. The canonical protein CRB1 isoform (NM_201253.2) consists of epidermal growth factor (EGF)-like domains, laminin AG-like domains, and a short cytoplasmic tail containing FERM- and PDZ-binding domains. There were 15 different variants found in this cohort, which have all been described previously.[24] The variant p.(Met1041Thr) was the most common variant, found in all 10 patients that originated from a Dutch genetic isolate and in 1 patient from outside the genetic isolate.

(IQR, 241.9; range, 17.7-739.2 mm^2) at baseline. Overall, there was no significant change in V4e seeing retinal areas at the 2-year follow-up visit (−3.5 mm^2; 95% CI, −17.4 to +10.3 mm^2; $P = .616$). A loss of ≥20% in V4e seeing retinal areas was seen in 7 eyes of 6 patients (16%), of whom 2 patients had BCVA-based severe visual impairment (BCVA ≤35 ETDRS letters). Moreover, 7 eyes of 4 patients showed an increase of ≥20% in V4e retinal seeing areas from baseline (Figure 2, B). These patients all had severe visual impairment based on visual acuity or visual fields (P20, central visual field <10° from point of fixation).

Microperimetry data were available for 36 of 44 eyes (82%). Microperimetry testing could not be reliably performed in a subset of patients due to age (patients P7 and P16) or severe visual impairment (P19, left eye; P20, both eyes). The left eye of patient P2 was also excluded because this eye was erroneously tested using different threshold settings at follow-up. Figure 3 shows representative microperimetry measurements performed in this cohort. Median BCEA 95% values were 32.9° ± 49.6° (range, 1.3°-187.4°) and 44.0° ± 49.7° (range, 1.0°-178.2°) for the right and left eyes, respectively.

Higher BCEA values, indicating a more unstable fixation, were seen in patients with worse logMAR BCVA (Spearman $\rho = 0.615$; $P = .004$). The mean macular sensitivity was 8.5 ± 7.6 dB (range, 0.0-24.3 dB) and 7.6 ± 7.5 dB (range, 0.0-26.3 dB) for right and left eyes, accordingly. Macular sensitivity correlated with logMAR BCVA (Spearman $\rho = -0.734$; $P < .001$). In 9 of 36 eyes (25%), macular sensitivity was ≤1 dB (Figure 3, patient P9). Analysis of the microperimetry testing grid (37 testing loci) showed that patients had a mean of 14.05 ± 12.02 loci (range, 0.0-34.0 loci) that showed no measurable sensitivity (0 dB; ie, absolute scotoma).

At follow-up, fixation stability was maintained (−14.9°; 95% CI, −35.7° to 5.0°; $P = .146$) (Figure 3, C). A significant loss of −1.7 dB (95% CI, −2.4 to −0.8 dB; $P < .001$) in macular sensitivity was observed after 2 years (Figure 3, D). This change was also seen after exclusion of eyes with significant cataract (−2.1 dB; 95% CI, −3.8 to −0.1; $P = .039$) or after exclusion of patients with a mean sensitivity of ≤1 dB (−2.1 dB; 95% CI, −3.1 to −1.1; $P < .001$). Additionally, there was a significant increase in testing loci with no measurable sensitivity (+3.5 loci; 95% CI, 0.4 to 6.5 loci; $P = .027$) at follow-up.

• **ERG AND FULL-FIELD STIMULUS TESTING:** Scotopic and photopic responses were minimal or nonrecordable at baseline in all patients with RP (Table). ERGs in P10 and P21 followed a CRD pattern, whereas P22 (the patient with a macular dystrophy phenotype) demonstrated full-field scotopic and photopic responses within normal limits. Patients with residual responses showed no significant changes in ERG patterns over follow-up. FST measurements were available for 14 patients (64%) at baseline and for 20 patients (91%) at follow-up because FST was not available at the start of this study. Two patients (P2 and P16) were not able to reliably perform FST, most likely due to young age. Therefore, to provide a more accurate and complete overview of FST measurements in this cohort, FST responses from the final visit were used for analysis. The mean thresholds for the white, blue, and red stimuli at last visit were −38.6 ± 12.5 dB (range, −57.0 to −11.9 dB), −42.7 ± 13.2 dB (range, −61.1 to −13.4 dB), and −26.3 ± 8.9 dB (range, −40.0 to −10.4 dB), respectively. Sensitivity thresholds for the white stimuli were best preserved in patients with mild RP and CRDs (Figure 4, A).

Based on the difference in thresholds between blue and red stimuli, FST responses in the 40 included eyes were rod-mediated in 15 (38%), mixed rod-cone mediated in 23 (57%), or cone-mediated in 2 (Figure 4, B). Cone-mediated responses could still be detected in both eyes of

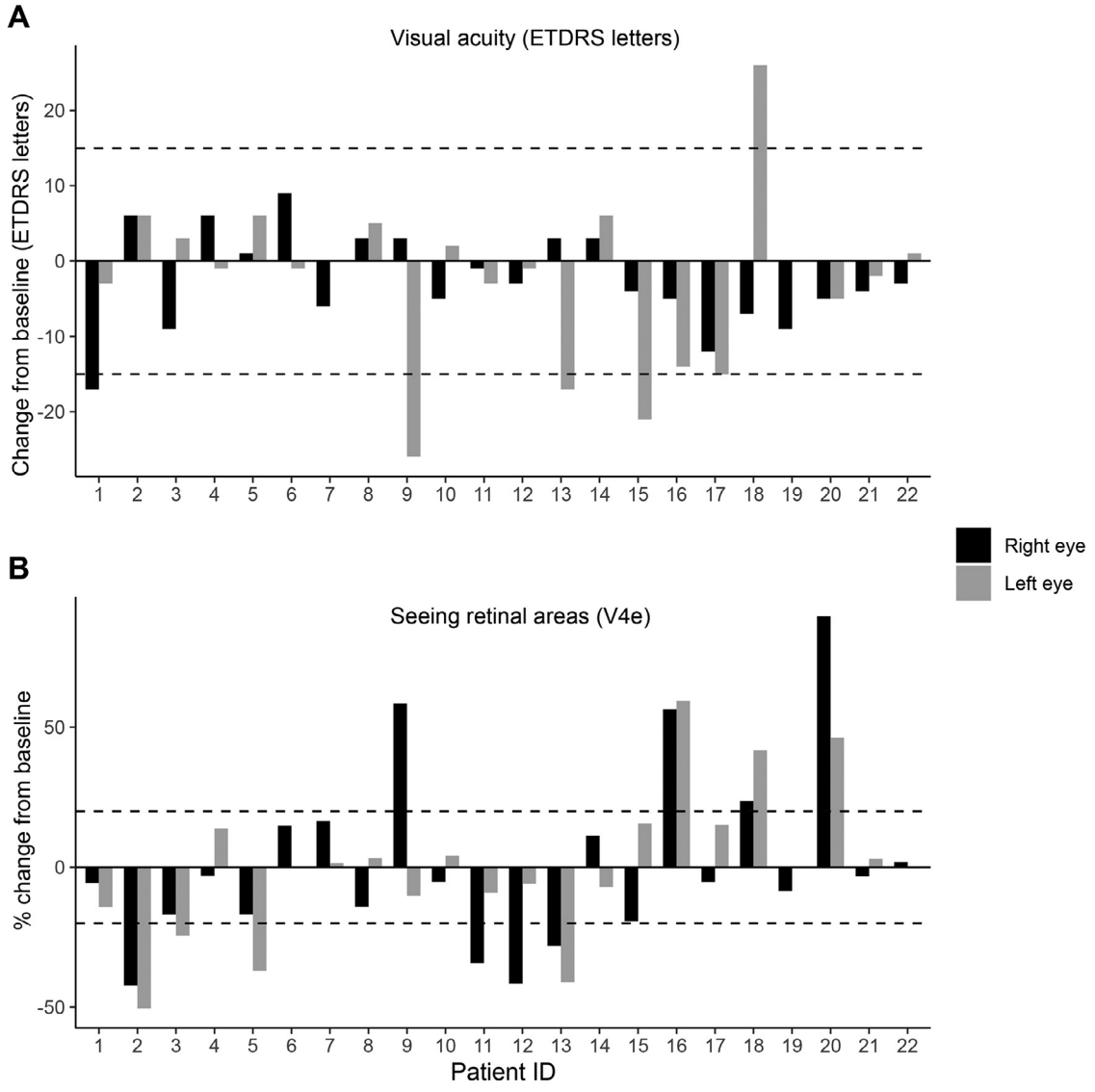

FIGURE 2. Changes in best-corrected visual acuity (BCVA) using Early Treatment Diabetic Retinopathy Study (ETDRS) letters and visual fields (retinal seeing areas, V4e stimuli) between baseline and 2-year follow-up are shown for each patient. Positive values reflect an improvement from baseline, whereas negative values signify a decrease from baseline. A. The absolute change in ETDRS letters was used to illustrate differences from baseline. The threshold for clinically significant BCVA changes was defined as a change of ≥15 ETDRS letters (dashed lines). B. For visual fields, the percentage change in retinal seeing areas was used, which was considered clinically significant if it exceeded a 20% change (dashed lines). Patients showing ≥20% improvement in visual field size had severe visual impairment (<35 ETDRS) or severely constricted visual fields (central diameter <20°).

patient P4 with early-onset RP, who had severe visual impairment and severely restricted visual fields. We were also able to determine FST responses in the left eye of patient P19 (light perception BCVA), who still had mixed FST responses but was nearing cone-mediated vision. In 14 of 20 patients (67%) with longitudinal FST data, we found no significant changes in white (−1.7 dB; 95% CI, −3.6 to 0.3 dB; $P = .098$), blue (−0.5 dB, 95% CI, −2.6 to 1.5 dB; $P = .610$), or red (−1.0 dB; 95% CI, −2.3 to 0.3 dB; $P = .132$) FST responses.

• **RETINAL IMAGING:** SD-OCT and FAF data were available in 21 of 22 patients (95%). Retinal imaging could not be performed in patient P16 with early-onset RP due to limited cooperation (aged 6) and nystagmus. A common observation seen on SD-OCT was retinal thickening, which was observed in 20 of 21 patients (95%). Cystoid macular edema and/or cystoid spaces were present in 14 eyes of 8 patients (38%) at baseline, which resolved completely in 4 eyes (28%) at follow-up without treatment. The mean central retinal thickness at baseline, after exclusion of patients with cystoid macular edema or cysts, was 133.0 ± 50.9

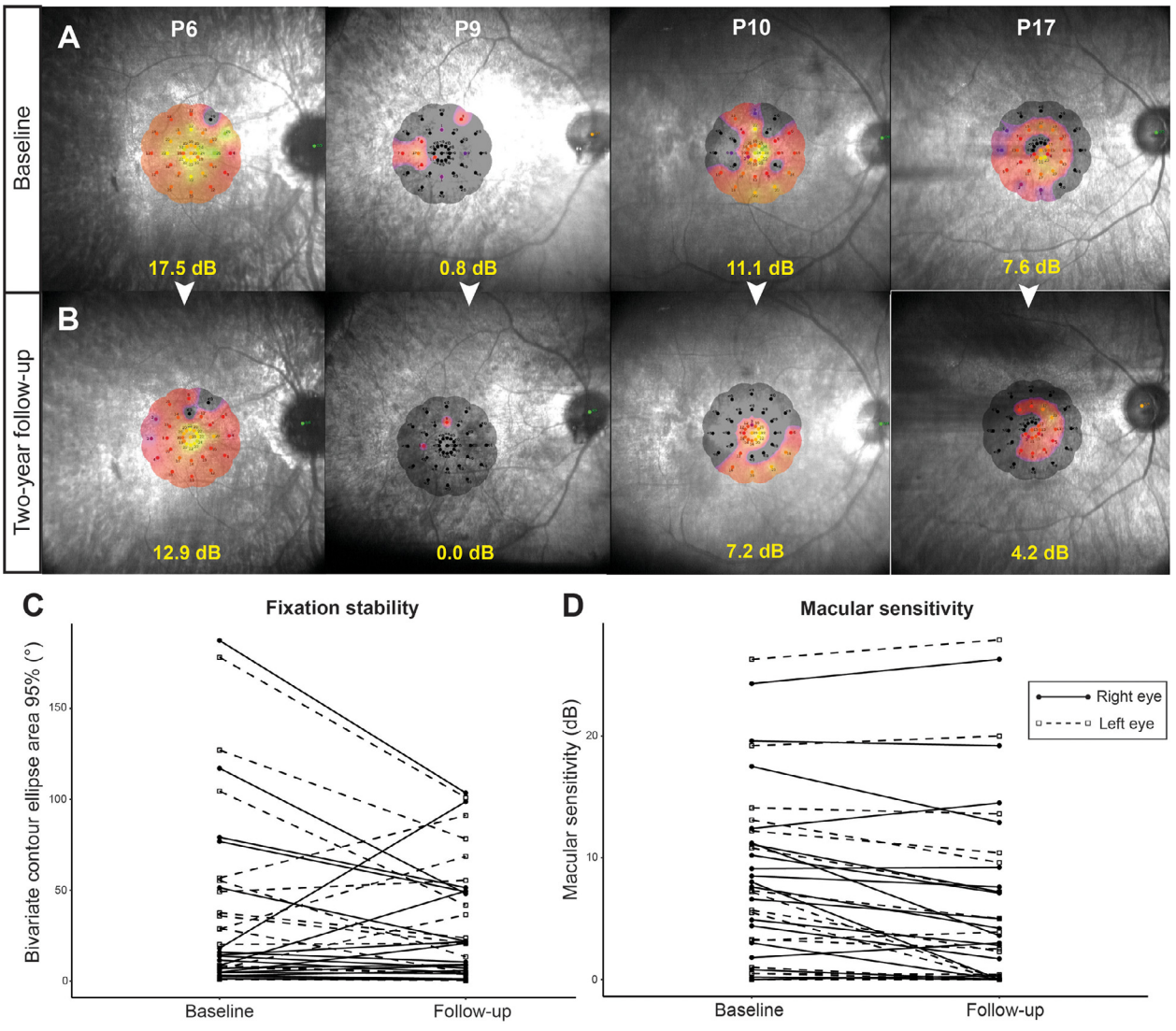

FIGURE 3. Macular sensitivity (MS) measurements on macular integrity assessment (MAIA) microperimetry in patients with crumbs cell polarity complex component 1 (*CRB1*)-associated retinal dystrophies. Color-coded heat maps demonstrate sensitivity values at each individual loci. Gray regions reflect areas where no sensitivity was measured (absolute scotomas). Mean MS values are shown in yellow. A. MS measurements at baseline in 4 patients with *CRB1*-associated retinal dystrophies. B. At the 2-year follow-up, MS loss was present in all 4 patients. Note that patient P17 was diagnosed with mild posterior subcapsular cataract, which may have contributed to MS loss measured on follow-up. C. A spaghetti plot shows longitudinal changes in fixation stability, using bivariate contour ellipse areas (BCEA), in all included study eyes (n = 36). Higher BCEA values signify a more unstable fixation. D. A spaghetti plot illustrates changes in MS for all included study eyes. A significant decline in MS was observed at the 2-year follow-up ($P < .001$).

μm (range, 59.5-236.0 μm), which did not significantly change at follow-up (−10.31 μm; 95% CI, −34.5 to 13.8 μm; $P = .371$).

The structure of the inner retina of patients was categorized into 3 different grades: (1) normal organization without coarse lamination in 5 (24%); (2) normal organization with coarse lamination in 8 (38%); and (3) relative disorganization with coarse lamination in 8 (38%) (Supplemental Figure and Supplemental Table 2). The hyperreflective outer retinal bands, ELM and EZ, were discontinuous or absent at the parafovea and perifovea in 18 of 21 patients (86%) (Supplemental Table 2). A degree of preservation of the ELM and EZ integrity was observed in patients with mild RP (P11 and P20) and in the patient with a macular dystrophy phenotype (P22). These 3 patients had better baseline logMAR BCVA (−0.6 logMAR; 95% CI, −1.1 to −0.1; $P = .015$) and macular sensitivity (+13.7 dB; 95% CI, 7.6 to 20.2 dB; $P < .001$) values compared with the other patients in this cohort. Qualitatively, there were no clear changes in ELM and EZ band integrity on SD-OCT imaging at the 2-year follow-up examinations, despite a decline in visual acuity in several patients (Figure 5). Because

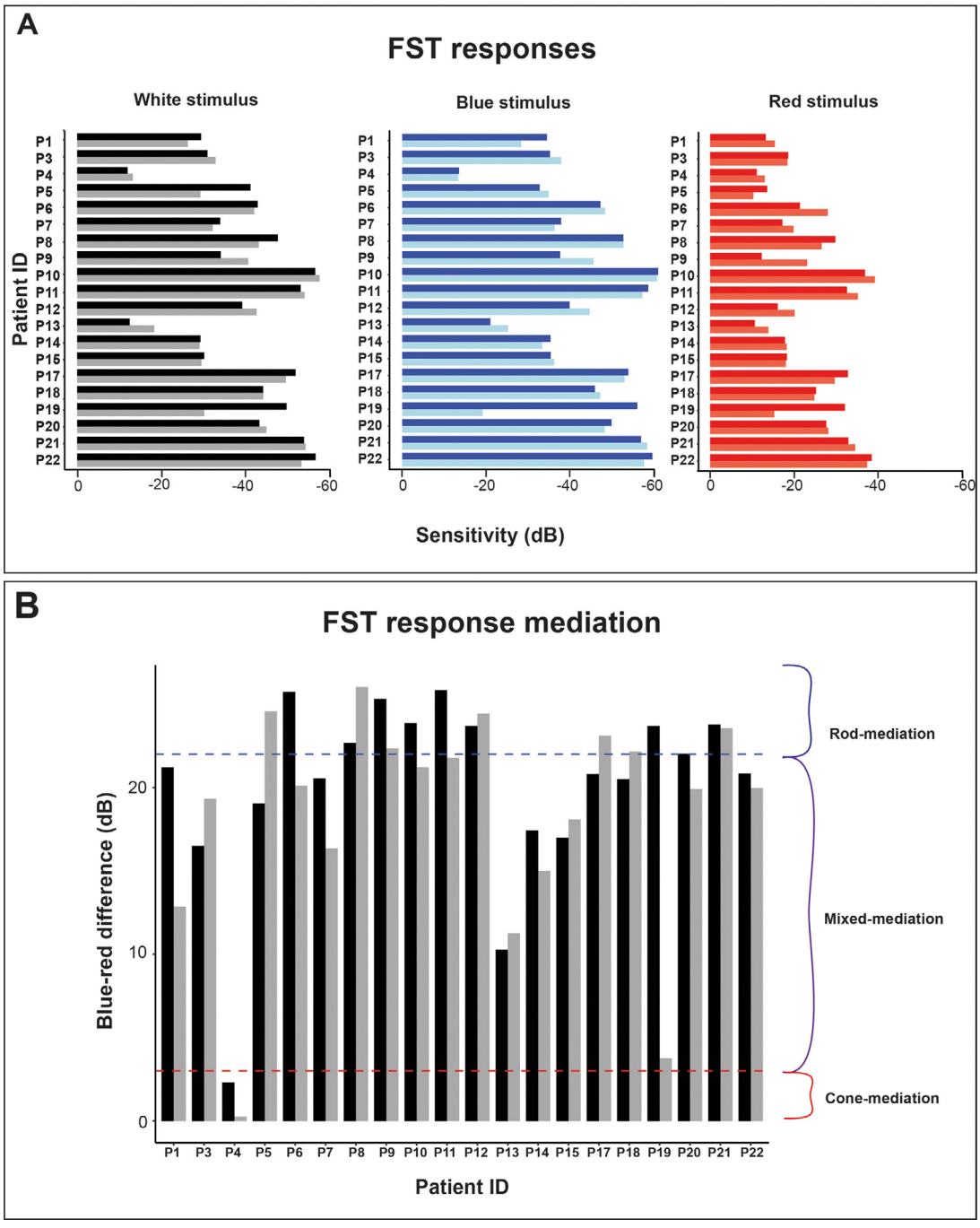

FIGURE 4. Full-field sensitivity thresholds (FST) responses obtained in 20 patients with crumbs cell polarity complex component 1 (*CRB1*)-associated retinal dystrophies at the 2-year follow-up. Two patients (P2 and P16) were unable to reliably perform FST testing due to young age. A. FST responses were obtained using white and chromatic stimuli (blue and red). The grouped bars represent the right eye (darker shaded bars) and left eyes (lighter shaded bars) of a single patient. B. Differences between blue and red responses were calculated for each patient. The blue-red difference determined whether FST responses were rod-mediated (difference of >22 dB), cone-mediated (difference <3 dB), or mixed rod- and cone-mediated (difference between 3 and 22 dB).

the integrity of ELM and EZ layers was severely affected in most of the patients (eg, Figure 5, A and B), quantitative analysis of the retinal bands could not be reliably performed.

On FAF imaging, the predominant pattern observed was generalized hypoautofluorescence in the midperipheral retina, with residual autofluorescence at the central macula, albeit to varying degrees (Figure 5, A). FAF imaging was also able to confirm our fundoscopic findings of preserved retinal pigment epithelium regions adjacent to retinal arterioles (Figure 5, B). Consistent with SD-OCT findings, aut-

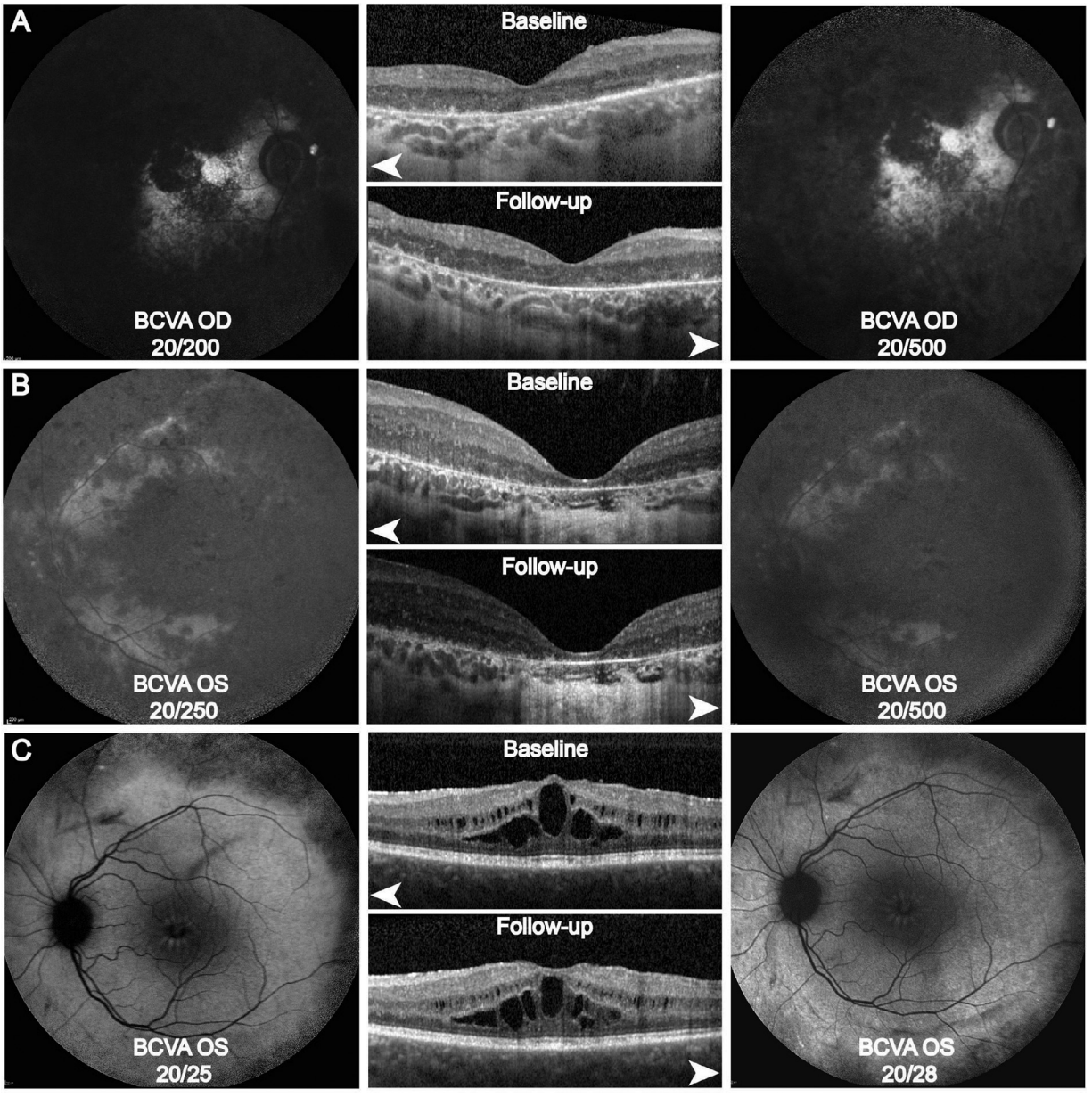

FIGURE 5. Patients P1, P13 and P11 with crumbs cell polarity complex component 1 (*CRB1*)-associated retinitis pigmentosa: Representative spectral-domain optical coherence tomography (SD-OCT) scans and corresponding fundus autofluorescence (FAF, white arrowheads) images at baseline and at 2-year follow-up. Best-corrected visual acuity (BCVA) is shown for each eye in Snellen notation. A. Patient P1, aged 30, showed characteristic features of a *CRB1* retina, including inner retinal thickening and coarse lamination of individual retinal layers. Outer retinal bands were nearly absent. FAF imaging in this patient showed overall absence of autofluorescence (AF) in the posterior pole, with some residual AF between the central macula and optic disc. B. Patient P13, aged 21, also showed retinal thickening and coarse lamination in addition to severe foveal atrophy. AF signals were nearly absent, with some preservation of retinal pigment epithelium alongside the vascular arterioles. C. Patient P11, aged 31, exhibited a mild form of retinitis pigmentosa. Unlike other retinitis pigmentosa patients in this cohort, the retinal structure of the inner and outer retina was retained, aside from the presence of cystoid macular edema. Consistent with SD-OCT findings, FAF imaging showed relative preservation of AF in the posterior pole, with signs of degeneration in the midperiphery.

ofluorescence signals were best preserved in patients with mild RP and macular dystrophy (Figure 5, C). The FAF patterns of each patient are described in Supplemental Table 2, which remained unchanged at follow-up.

DISCUSSION

In this prospective natural history study, we evaluated the functional and structural changes in patients with biallelic

TABLE. Summary of the Clinical Characteristics of Patients With Crumbs Cell Polarity Complex Component 1-Associated Retinal Dystrophies at Last Examination.

Characteristic	Total (N = 22)
Age, y	
Mean ± SD	29.3 ± 16.0
Median (IQR)	27.8 (19.4)
Range	8.3-76.9
Sex, n (%)	
Female	13 (59)
Male	9 (41)
Clinical diagnosis, n (%)	
Retinitis pigmentosa	19 (86)
Cone-rod dystrophy	2 (9)
Macular dystrophy	1 (5)
Age at onset, y	
Mean ± SD	8.2 ± 11.9
Median (IQR)	3.0 (7.8)
Range	0.8-49.0
Initial symptoms, n (%)	
Nyctalopia	5 (23)
Visual field loss	8 (36)
Visual acuity loss	7 (32)
Nystagmus	2 (9)
Disease duration, y	
Mean ± SD	19.0 ± 10.7
Median (IQR)	18.7 (16.7)
Range	4.7-39.3
Best-corrected visual acuity in ETDRS	
Mean ± SD	38.6 ± 19.7
Median (IQR)	35.8 (27.1)
Range	8.5-76.5
SER, diopters	
Mean ± SD	2.2 ± 2.9
Median (IQR)	2.4 (3.9)
Range	−5.9 to 6.7
Axial length, mm^2	
Mean ± SD	21.1 ± 1.7
Median (IQR)	20.8 (1.7)
Range	19.0-26.3
V4e isopter seeing retinal areas, mm^2	
Mean ± SD	258.6 ± 230.9
Median (IQR)	189.4 (261.7)
Range	14.5-744.4
Electroretinography patterns, n (%)	
Normal responses	1 (5)
Cone-rod pattern	2 (9)
Minimal responses	1 (5)
Nondetectable	18 (81)

ETDRS = Early Treatment Diabetic Retinopathy Study, IQR = interquartile range, SER = spherical equivalent of the refractive error.

Findings were averaged between eyes.

CRB1 variants causing a spectrum of RDs, as we anticipate the start of gene therapeutic trials for *CRB1*-associated RDs in the near future. Our 2-year analysis of the cohort showed that visual acuity and visual fields did not significantly change during follow-up. BCVA and visual fields are parameters with relatively low sensitivity for early disease changes and may not be suitable as primary outcome measures in clinical trials investigating diseases, such as RP, that have relatively slow progression rates.[33] Still, in 5 eyes of 5 different patients, aged between 22 and 31 years, we found a BCVA loss of >15 ETDRS letters (equivalent to +0.3 logMAR), which is considered a clinically significant change in clinical trials and by regulatory agencies.[34,35]

This finding suggests a faster decline around the third decade of life, although the contribution of significant cataract, which was the case for 2 of 5 eyes, should not be disregarded. This is in line with our retrospective natural history study, which reported median ages of 18, 32, and 44 years to reach moderate visual impairment, severe visual impairment, and blindness, respectively.[18] Based on BCVA data, we suggest that the optimal window for treatment is before the third decade of life. Ideally, patients should be treated at the earliest and safest opportunity to gain the most benefit from gene therapy.

Regarding visual fields, we found that 7 eyes of 6 patients showed progression within the 2-year follow-up period, defined as a loss of ≥20% of the seeing retinal area, which is the test-retest limit in patients with RP as found by Bittner and associates.[26] However, these changes should be interpreted with caution, because greater variability in visual field measurements is predicted in patients with more advanced stages of BCVA-based or visual field-based impairment.[36-38] This is evidently demonstrated in our cohort, as 4 severe visually impaired patients showed improvements up to 90% in visual fields areas at follow-up, in absence of intervention.

Goldmann kinetic perimetry assumes stable and foveal fixation, which is not always the case in patients with severe RP such as in the current study.[26] Instead, other perimetry measurements, such as semiautomated kinetic perimetry or wide-field static perimetry, could be used in future studies for peripheral visual field assessment, because they take fixation stability into consideration and limit operator-dependent variability.[39]

Fundus-tracking perimetry, also known as microperimetry, is a commonly used tool for monitoring disease progression and for assessing treatment efficacy in trials involving other RDs, such as Stargardt disease, choroideremia, and X-linked RP.[32,40-42] In these RDs, subtle changes in the retina over short periods of time were detectable on microperimetry, preceding detection on conventional parameters.[27,43] Similar results were found in our cohort, in which we detected a significant decline in macular sensitivity between visits, while no significant decline in BCVA was detected in the 2-year period.

Thus, microperimetry is a sensitive progression marker and has the potential to serve as a clinical end point in treat-

ment trials for *CRB1*-associated RD. However, due to the subjective nature of psychophysical metrics, measurements on microperimetry are inherently susceptible to variability, which is affected by factors including age, the type of retinal disease, disease severity, learning effects, and natural variance.[27,44] Our study accounted for potential learning effects, but formal intrasession and intersession reliability testing was not performed. Because the main goal of phase III gene therapy trials is treatment efficacy, a patient's ability to reliably perform microperimetry testing could potentially be an inclusion criterion.

Analysis of microperimetry was also impeded by the increasing amount of absolute scotoma points, which resulted in nearly undetectable sensitivity thresholds (macular sensitivity ≤1 dB) in 9 out of 36 study eyes (25%). Reporting the macular sensitivity, which is calculated using the average sensitivity of all testing loci, may not be an ideal approach, because this underestimates the change occurring in individual loci with detectable sensitivity.[27,40,45] Other methods that investigate regional sensitivity changes, along with test-retest reliability testing, should be explored in future studies.[44]

On electrophysiological testing, ERG responses were nonrecordable in most of the RP patients, implying that full-field ERG has no value in monitoring disease progression in patients with *CRB1*-associated RP. An alternative approach to assess residual photoreceptor function is the measurement of sensitivity thresholds using FST, which can be performed regardless of fixation capabilities or ERG function.[46] FST testing showed rod or mixed responses in this cohort, which shows that functional photoreceptors are still present despite this severe early-onset disease. Cone-mediated responses were found in patient P4, which is suggestive for end-stage disease because these responses are typically found in patients with an LCA phenotype.[13,47] As such, FST can provide valuable knowledge on remaining photoreceptor function, and in turn, disease severity, which can guide the selection of eligible candidates for therapeutic intervention.[32] However, FST responses do not appear to be sensitive markers for disease progression over a relatively short period given that we found no significant changes in FST responses over the course of 2 years. Small, localized changes occurring over several years possibly go unnoticed, because FST measures the sensitivity of the entire retina, without revealing spatial information.[30] Nevertheless, FST is potentially capable of measuring a treatment effect, as shown in previous gene therapy trials, and should be considered as a clinical end point.[48-50]

In keeping with previous studies, SD-OCT imaging in patients with *CRB1*-associated RP revealed an abnormally thickened inner retina (95%), which could be accompanied by coarse lamination of inner retinal layers and/or cystoid macular edema.[11,17,18] The loss of CRB1 function has been postulated to stimulate proliferation of retinal progenitor cells and also disrupt naturally occurring apoptosis during retinal development.[9,17] This phenomenon is in direct contrast with other molecular forms of RP/LCA, where progressive thinning of the inner retinal layers typically occurs.[51] Regardless of inner retinal thickening, 13 out of 21 patients (62%) showed a relatively preserved laminar organization, which may be amenable for gene therapy treatment.

The hyperreflective retinal bands, ELM and EZ, were typically discontinuous or indiscernible, consistent with FAF findings, owing to the rapid disease progression at an early age in *CRB1*-associated RP, which impeded quantitative analysis.[51] Despite the state of the inner and outer retina, retinal sensitivity could still be measured using psychophysical metrics, indicating that SD-OCT findings do not necessarily reflect remaining photoreceptor function in patients with *CRB1*-associated RDs.

There is an urgent need for reliable methods for accurate quantification and localization of remaining photoreceptors, because viable photoreceptors are a prerequisite for effective treatment with gene therapy.[52-54] A potential method is the use of adaptive optics because it allows for the assessment of photoreceptor viability on a cellular level, which, in turn, can shed light on their amenability for gene therapy treatment.[54-56] It would be of great interest to assess in future studies whether photoreceptors can be adequately identified using adaptive optics considering the severe, early-onset degeneration and the characteristic retinal phenotype seen in *CRB1* patients.

Our study has several limitations. We included a relatively small cohort of 22 patients with *CRB1*-associated RDs, which limited the possibility of a more in-depth subgroup analysis. Furthermore, patients were observed for a 2-year period, so it is possible that parameters with low sensitivity for disease progression in our current study, such as visual acuity and FST, will be able to demonstrate progression over a longer observation period.

Novel outcome measurements used in the assessment of gene therapy, such as multiluminance mobility tests, dark-adapted chromatic perimetry and pupil campimetry, were also not assessed in this study.[57,58]

Future studies that monitor a large group of patients with *CRB1* variants over a longer period of time, while also assessing the feasibility of more recent outcome measures, would be invaluable to extend our current findings.

In conclusion, this is the first prospective natural history study performed in patients with RDs associated with biallelic *CRB1* variants. Our study discusses the feasibility of commonly used outcome measures as clinical end points in clinical trials and their potential caveats. BCVA and visual fields measures show stability over 2 years and need to be complemented with more sensitive progression markers. Microperimetry and FST show the most potential as clinical end points, but further investigation into their reliability, validity, and feasibility is required. The findings in this study can be used to aid the design of interventional studies, paving the way for *CRB1* gene therapy trials in the near future.

Funding/Support: This research was supported by Algemene Nederlandse Vereniging ter Voorkoming van Blindheid (ANVVB), Landelijke Stichting voor Blinden en Slechtzienden (LSBS), and the Oogfonds, which contributed through UitZicht (Delft, the Netherlands), as well as the Curing Retinal Blindness Foundation, Stichting Blindenhulp, Bontius Stichting, and Retina Fonds. These funding organizations had no role in the design or conduct of this research.

Financial Disclosures: Leiden University Medical Center is the holder of patent application PCT/NL2014/050549, which describes the potential clinical use of CRB2. Jan Wijnholds is listed as inventor on this patent and is an employee of Leiden University Medical Center. The other authors indicate no financial support or conflicts of interest. All authors attest that they meet the current ICMJE criteria for authorship.

Acknowledgments: : L. Ingeborgh van den Born, Carel B. Hoyng, and Camiel J.F. Boon are members of the European Reference Network for Rare Eye diseases (ERN-EYE).

REFERENCES

1. Khan KN, Robson A, Mahroo OAR, et al. A clinical and molecular characterisation of CRB1-associated maculopathy. *Eur J Hum Genet*. 2018;26(5):687–694.
2. Vincent A, Ng J, Gerth-Kahlert C, et al. Biallelic mutations in *CRB1* underlie autosomal recessive familial foveal retinoschisis. *Invest Ophthalmol Vis Sci*. 2016;57(6):2637–2646.
3. Lotery AJ, Jacobson SG, Fishman GA, et al. Mutations in the CRB1 gene cause Leber congenital amaurosis. *Arch Opthalmol*. 2001;119(3):415–420.
4. den Hollander AI, Heckenlively JR, van den Born LI, et al. Leber congenital amaurosis and retinitis pigmentosa with Coats-like exudative vasculopathy are associated with mutations in the crumbs homologue 1 (*CRB1*) gene. *Am J Hum Genet*. 2001;69(1):198–203.
5. Verbakel SK, van Huet RAC, Boon CJF, et al. Non-syndromic retinitis pigmentosa. *Prog Retin Eye Res*. 2018;66:157–186.
6. Hartong DT, Berson EL, Dryja TP. Retinitis pigmentosa. *Lancet*. 2006;368(9549):1795–1809.
7. Quinn PM, Buck TM, Mulder AA, et al. Human iPSC-derived retinas recapitulate the fetal CRB1 CRB2 complex formation and demonstrate that photoreceptors and Müller glia are targets of AAV5. *Stem Cell Reports*. 2019;12(5):906–919.
8. Quinn PM, Pellissier LP, Wijnholds J. The CRB1 complex: following the trail of crumbs to a feasible gene therapy strategy. *Front Neurosci*. 2017;11:175.
9. Alves CH, Pellissier LP, Wijnholds J. The CRB1 and adherens junction complex proteins in retinal development and maintenance. *Prog Retin Eye Res*. 2014;40:35–52.
10. Boon N, Wijnholds J, Pellissier LP. Research models and gene augmentation therapy for *CRB1* retinal dystrophies. *Front Neurosci*. 2020;14:860.
11. Bujakowska K, Audo I, Mohand-Saïd S, et al. *CRB1* mutations in inherited retinal dystrophies. *Hum Mutat*. 2012;33(2):306–315.
12. Ray TA, Cochran K, Kozlowski C, et al. Comprehensive identification of mRNA isoforms reveals the diversity of neural cell-surface molecules with roles in retinal development and disease. *Nat Commun*. 2020;11(1) 3328-3328.
13. Stingl KT, Kuehlewein L, Weisschuh N, et al. Chromatic full–field stimulus threshold and pupillography as functional markers for late-stage, early-onset retinitis pigmentosa caused by *CRB1* mutations. *Transl Vis Sci Technol*. 2019;8(6).
14. Alves CH, Boon N, Mulder AA, Koster AJ, Jost CR, Wijnholds J. CRB2 loss in rod photoreceptors is associated with progressive loss of retinal contrast sensitivity. *Int J Mol Sci*. 2019;20(17):4069.
15. Pellissier LP, Quinn PM, Alves CH, et al. Gene therapy into photoreceptors and Müller glial cells restores retinal structure and function in CRB1 retinitis pigmentosa mouse models. *Hum Mol Genet*. 2015;24(11):3104–3118.
16. Mehalow AK, Kameya S, Smith RS, et al. *CRB1* is essential for external limiting membrane integrity and photoreceptor morphogenesis in the mammalian retina. *Hum Mol Genet*. 2003;12(17):2179–2189.
17. Jacobson SG, Cideciyan AV, Aleman TS, et al. Crumbs homolog 1 (*CRB1*) mutations result in a thick human retina with abnormal lamination. *Hum Mol Genet*. 2003;12(9):1073–1078.
18. Talib M, van Schooneveld MJ, van Genderen MM, et al. Genotypic and phenotypic characteristics of *CRB1*-associated retinal dystrophies. *Ophthalmology*. 2017;124(6):884–895.
19. Buck TM, Vos RM, Alves CH, Wijnholds J. AAV-*CRB2* protects against vision loss in an inducible *CRB1* retinitis pigmentosa mouse model. *Mol Ther Methods Clin Dev*. 2021;20:423–441.
20. Talib M, Boon CJF. Retinal dystrophies and the road to treatment: clinical requirements and considerations. *Asia Pac J Ophthalmol (Phila)*. 2020;9(3):159–179.
21. Mathijssen IB, Florijn RJ, van den Born LI, et al. Long-term follow-up of patients with retinitis pigmentosa type 12 caused by *CRB1* mutations: a severe phenotype with considerable interindividual variability. *Retina*. 2017;37(1):161–172.
22. van Huet RAC, Oomen CJ, Plomp AS, et al. The RD5000 Database: facilitating clinical, genetic, and therapeutic studies on inherited retinal diseases. *Invest Ophthalmol Vis Sci*. 2014;55(11):7355–7360.
23. van den Born LI, van Soest S, van Schooneveld MJ, Riemslag FCC, de Jong PTVM, Bleeker-Wagemakers EM. Autosomal recessive retinitis pigmentosa with preserved para-arteriolar retinal pigment epithelium. *Am J Ophthalmol*. 1994;118(4):430–439.
24. Talib M, van Schooneveld MJ, Wijnholds J, et al. Defining inclusion criteria and endpoints for clinical trials: a prospective cross-sectional study in *CRB1*-associated retinal dystrophies. *Acta Ophthalmol*. 2021;99(3):e402–e414.
25. Dagnelie G. Technical note. Conversion of planimetric visual field data into solid angles and retinal areas. *Clin Vision Sci*. 1990;5(1):95–100.
26. Bittner AK, Iftikhar MH, Dagnelie G. Test-retest, within-visit variability of Goldmann visual fields in retinitis pigmentosa. *Invest Ophthalmol Vis Sci*. 2011;52(11):8042–8046.
27. Wu Z, Ayton LN, Guymer RH, Luu CD. Intrasession test–retest variability of microperimetry in age-re-

lated macular degeneration. *Invest Ophthalmol Vis Sci*. 2013;54(12):7378–7385.
28. Talib M, Jolly JK, Boon CJF. Measuring central retinal sensitivity using microperimetry. In: Boon CJF, Wijnholds J, eds. Retinal Gene Therapy: Methods and Protocols. New York: Springer; 2018:339–349.
29. Roman AJ, Cideciyan AV, Aleman TS, Jacobson SG. Full–field stimulus testing (FST) to quantify visual perception in severely blind candidates for treatment trials. *Physiol Meas*. 2007;28(8):N51–N56.
30. Roman AJ, Schwartz SB, Aleman TS, et al. Quantifying rod photoreceptor-mediated vision in retinal degenerations: dark-adapted thresholds as outcome measures. *Exp Eye Res*. 2005;80(2):259–272.
31. Klein M, Birch DG. Psychophysical assessment of low visual function in patients with retinal degenerative diseases (RDDs) with the Diagnosys full-field stimulus threshold (D-FST). *Doc Ophthalmol*. 2009;119(3):217.
32. Dimopoulos IS, Tseng C, MacDonald IM. Microperimetry as an outcome measure in choroideremia trials: reproducibility and beyond. *Invest Ophthalmol Vis Sci*. 2016;57(10):4151–4161.
33. Fishman GA, Jacobson SG, Alexander KR, et al. Outcome measures and their application in clinical trials for retinal degenerative diseases: outline, review, and perspective. *Retina*. 2005;25(6):772–777.
34. Lam BL, Feuer WJ, Schiffman JC, et al. Trial end points and natural history in patients with G11778A Leber hereditary optic neuropathy: preparation for gene therapy clinical trial. *JAMA Ophthalmol*. 2014;132(4):428–436.
35. Kiser AK, Mladenovich D, Eshraghi F, Bourdeau D, Dagnelie G. Reliability and consistency of visual acuity and contrast sensitivity measures in advanced eye disease. *Optom Vis Sci*. 2005;82(11):946–954.
36. Barnes CS, Schuchard RA, Birch DG, et al. Reliability of semiautomated kinetic perimetry (SKP) and Goldmann kinetic perimetry in children and adults with retinal dystrophies. *Transl Vis Sci Technol*. 2019;8(3) 36-36.
37. Barry MP, Bittner AK, Yang L, Marcus R, Iftikhar MH, Dagnelie G. Variability and errors of manually digitized Goldmann visual fields. *Optom Vis Sci*. 2016;93(7):720–730.
38. Roman AJ, Cideciyan AV, Schwartz SB, Olivares MB, Heon E, Jacobson SG. Intervisit variability of visual parameters in Leber congenital amaurosis caused by *RPE65* mutations. *Invest Ophthalmol Vis Sci*. 2013;54(2):1378–1383.
39. Kumaran N, Rubin GS, Kalitzeos A, et al. A cross–sectional and longitudinal study of retinal sensitivity in *RPE65*-associated Leber congenital amaurosis. *Invest Ophthalmol Vis Sci*. 2018;59(8):3330–3339.
40. Schönbach EM, Strauss RW, Muñoz B, et al. Longitudinal microperimetric changes of macular sensitivity in Stargardt disease after 12 months: ProgStar Report No. 13. *JAMA Ophthalmol*. 2020;138(7):772–779.
41. Georgiou M, Singh N, Kane T, et al. Long-term investigation of retinal function in patients with achromatopsia. *Invest Ophthalmol Vis Sci*. 2020;61(11) 38-38.
42. Buckley TMW, Jolly JK, Menghini M, Wood LJ, Nanda A, MacLaren RE. Test-retest repeatability of microperimetry in patients with retinitis pigmentosa caused by mutations in RPGR. *Clin Exp Ophthalmol*. 2020;48(5):714–715.
43. Jolly JK, Xue K, Edwards TL, Groppe M, MacLaren RE. Characterizing the natural history of visual function in choroideremia using microperimetry and multimodal retinal imaging. *Invest Ophthalmol Vis Sci*. 2017;58(12):5575–5583.
44. Pfau M, Jolly JK, Wu Z, et al. Fundus-controlled perimetry (microperimetry): application as outcome measure in clinical trials. *Prog Retin Eye Res*. 2021;82:100907.
45. Iftikhar M, Kherani S, Kaur R, et al. Progression of retinitis pigmentosa as measured on microperimetry: The PREP-1 Study. *Ophthalmol Retina*. 2018;2(5):502–507.
46. Maguire AM, High KA, Auricchio A, et al. Age-dependent effects of *RPE65* gene therapy for Leber's congenital amaurosis: a phase 1 dose-escalation trial. *Lancet*. 2009;374(9701):1597–1605.
47. Collison FT, Park JC, Fishman GA, McAnany JJ, Stone EM. Full-field pupillary light responses, luminance thresholds, and light discomfort thresholds in *CEP290* Leber congenital amaurosis patients. *Invest Ophthalmol Vis Sci*. 2015;56(12):7130–7136.
48. Russell S, Bennett J, Maguire AM, High KA. Voretigene neparvovec-rzyl for the treatment of biallelic *RPE65* mutation–associated retinal dystrophy. *Expert Opin Orphan Drugs*. 2018;6(8):457–464.
49. Russell S, Bennett J, Wellman JA, et al. Efficacy and safety of voretigene neparvovec (AAV2-hRPE65v2) in patients with *RPE65*-mediated inherited retinal dystrophy: a randomised, controlled, open-label, phase 3 trial. *Lancet*. 2017;390(10097):849–860.
50. Klein M, Mejia P, Galles D, Birch DG. Full-field stimulus thresholds (FSTs) in subjects with inherited retinal degenerations (IRDs)—a 10 years review. *Invest Ophthalmol Vis Sci*. 2018;59(9) 54-54.
51. Tee JJL, Yang Y, Kalitzeos A, Webster A, Bainbridge J, Michaelides M. Natural history study of retinal structure, progression, and symmetry using ellipzoid zone metrics in *RPGR*-associated retinopathy. *Am J Ophthalmol*. 2019;198:111–123.
52. Gardiner KL, Cideciyan AV, Swider M, et al. Long-term structural outcomes of late-stage *RPE65* gene therapy. *Mol Ther*. 2020;28(1):266–278.
53. Aguirre GD. Concepts and strategies in retinal gene therapy. *Invest Ophthalmol Vis Sci*. 2017;58(12):5399–5411.
54. Georgiou M, Kalitzeos A, Patterson EJ, Dubra A, Carroll J, Michaelides M. Adaptive optics imaging of inherited retinal diseases. *Br J Ophthalmol*. 2018;102(8):1028–1035.
55. Genead MA, Fishman GA, Rha J, et al. Photoreceptor structure and function in patients with congenital achromatopsia. *Invest Ophthalmol Vis Sci*. 2011;52(10):7298–7308.
56. Georgiou M, Fujinami K, Michaelides M. Inherited retinal diseases: therapeutics, clinical trials and end points—a review. *Clin Exp Ophthalmol*. 2021;49(3):270–288.
57. Stingl K, Kempf M, Bartz-Schmidt KU, et al. Spatial and temporal resolution of the photoreceptors rescue dynamics after treatment with voretigene neparvovec. *Br J Ophthalmol*. 2021 Published online January 20. doi:10.1136/bjophthalmol-2020-318286.
58. Maguire AM, Russell S, Wellman JA, et al. Efficacy, safety, and durability of voretigene neparvovec-rzyl in *RPE65* mutation–associated inherited retinal dystrophy: results of phase 1 and 3 trials. *Ophthalmology*. 2019;126(9):1273–1285.